Supporting material for "Microscopic interplay of temperature and disorder of a 1D elastic interface"

Nirvana Caballero,[1,*] Thierry Giamarchi,[1] Vivien Lecomte,[2] and Elisabeth Agoritsas[3]

[1] *Department of Quantum Matter Physics, University of Geneva, 24 Quai Ernest-Ansermet, CH-1211 Geneva, Switzerland*

[2] *Université Grenoble Alpes, CNRS, LIPhy, FR-38000 Grenoble, France*

[3] *Institute of Physics, Ecole Polytechnique Fédérale de Lausanne (EPFL), CH-1015 Lausanne, Switzerland*

(Dated: October 26, 2021)

CONTENTS

I. PINNING FORCE CORRELATOR AND DISORDER STRENGTH

In this section, we detail how we generate the quenched random potential $V_p(y,u)$ and its associated pinning force $F_p(y,u) \equiv -\partial_u V_p(y,u)$. We recall that the interface is parametrized by the univalued displacement field $u(y,t)$, with the internal coordinate y taking discrete values $y = j\Delta y$ (where j is an integer, $j = 0, \dots L_y/\Delta y$), and the transverse coordinate u taking continuous values. We consider a disorder with Gaussian distribution fully characterized by a zero mean and the two-point correlators:

$$\begin{aligned} \overline{V_p(y_1,u_1)V_p(y_2,u_2)} &= D\, R_\xi(u_2-u_1)\,\delta_{y_2 y_1}\,, \\ \overline{F_p(y_1,u_1)F_p(y_2,u_2)} &= \Delta_\xi(u_2-u_1)\,\delta_{y_2 y_1}\,, \end{aligned} \tag{1}$$

where $\overline{\cdots}$ denotes the average over disorder realizations. We chose the normalization $\int_{\mathbb{R}} \mathrm{d}u\, R_\xi(u) = 1$, and the correlators are simply related by $\Delta_\xi(u) = -D R''_\xi(u)$. In the following, we thus make explicit the functional $\Delta_\xi(u)$ and the disorder strength D.

* Corresponding author: Nirvana.Caballero@unige.ch

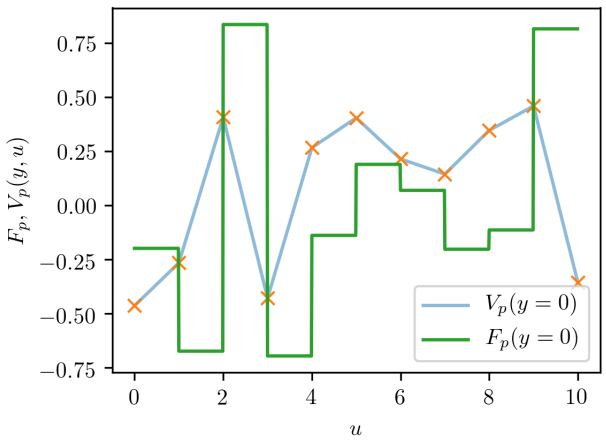

Figure 1. For a fixed coordinate y, the random potential $V_p(y,u)$ is generated by a linear interpolation between random numbers taken from a uniform distribution with zero mean (orange crosses). The associated pinning force F_p is obtained from the associated piecewise derivative $F_p(y,u) = -\partial_u V_p(y,u)$.

A. Generating a spatially-correlated disorder

The pinning potential $V_p(y,u)$ is defined independently for each discrete value of the coordinate y, so that in what follows, one fixes y and considers only the coordinate u. The procedure to generate the corresponding quenched 'landscape' $U(u) \equiv V_p(y,u)$ at fixed y, spatially-correlated with a finite correlation length ξ, is the following (see Fig. 1). We first discretize the direction u with fixed steps $\Delta u = \xi$. A random number U_k is generated independently at each site $u = k\Delta u$ (with k an integer) from a probability distribution function $\mathcal{P}(U_k)$ of zero mean.

Then, on every interval $u \in [k\Delta u, (k+1)\Delta u]$ (*i.e.* one has $k = \lfloor u/\Delta u \rfloor$) the random pinning potential is defined as a linear interpolation between U_k and U_{k+1}:

$$U(u) = U_k + \frac{U_{k+1} - U_k}{\Delta u}(u - k\Delta u)\,. \tag{2}$$

One can easily check that, as required, this definition satisfies $U(k\Delta u) = U_k$ and $U((k+1)\Delta u) = U_{k+1}$. The associated pinning force $F_p(u) = -\partial_u U(u)$ is finally

given by the discrete derivative

$$F_p(u) = -\frac{U_{k+1} - U_k}{\Delta u} \tag{3}$$

with $k = \lfloor u/\Delta u \rfloor$ as above.

For our simulations we sort each reference value U_k from a *uniform* distribution on the interval $[-\frac{\epsilon}{2}, \frac{\epsilon}{2}]$, with $\epsilon > 0$. It has consequently a zero mean and a variance

$$D_0 \equiv \overline{(U_k)^2} = \frac{\epsilon^2}{12}\,. \tag{4}$$

To keep the discussion general, thereafter we generically denote the variance of U_k as a control parameter D_0. In addition, we discuss in Sec. III how choosing an alternative distribution $\mathcal{P}(U_k)$ (non-uniform but with the same variance) leads to physically consistent results.

B. Piecewise linear force correlator

We start by defining the intermediate two-point correlator of the force as

$$\Delta_\xi^{(2)}(u_1, u_2) = \overline{F_p(u_1) F_p(u_2)}\,. \tag{5}$$

Because it is associated to the specific set of intervals $u \in [k\Delta u, (k+1)\Delta u]$ with $k = \lfloor u/\Delta u \rfloor$, it is important to notice that it is *not* invariant by translation along the u direction. Indeed, pairs of points (u_1, u_2) separated by a same distance $u = u_2 - u_1$ can either lie in the same interval $[k\Delta u, (k+1)\Delta u]$ or not.

One has in fact three possibilities: if (u_1, u_2) are

- in the same interval, one has

$$\Delta_\xi^{(2)}(u_1, u_2) = 2\overline{(U_i)^2} = \frac{2D_0}{\Delta u^2}\,; \tag{6}$$

- in adjacent intervals $[(k-1)\Delta u, k\Delta u]$ and $[k\Delta u, (k+1)\Delta u]$:

$$\Delta_\xi^{(2)}(u_1, u_2) = -\overline{(U_i)^2} = -\frac{D_0}{\Delta u^2}\,; \tag{7}$$

- in more distant intervals $[k\Delta u, (k+1)\Delta u]$ and $[j\Delta u, (j+1)\Delta u]$ with $|k - j| \leq 2$:

$$\Delta_\xi^{(2)}(u_1, u_2) = 0\,. \tag{8}$$

And from now on we use that $\xi = \Delta u$ to emphasize the explicit dependence on the correlation length ξ.

To recover a translation-invariant correlator, as required in the definitions (1), one must average the intermediate correlator $\Delta_\xi^{(2)}(u_1, u_2)$ over all pairs of points (u_1, u_2) separated by the same distance u:

$$\Delta_\xi(u) = \int_{\mathbb{R}^2} \mathrm{d}u_1 \mathrm{d}u_2\, \delta(u_2 - u_1 - u)\, \Delta_\xi^{(2)}(u_1, u_2)\,. \tag{9}$$

One finds by an explicit computation

$$\Delta_\xi(u) = \frac{D_0}{\xi^2}\, \Delta_{\mathrm{adim}}\big(u/\xi\big) \tag{10}$$

with $\Delta_{\mathrm{adim}}(\hat{u})$ the piecewise linear continuous function that connects the values:

$$\Delta_{\mathrm{adim}}(\hat{u}) = 2 \quad \text{for} \quad \hat{u} = 0\,, \tag{11}$$
$$\Delta_{\mathrm{adim}}(\hat{u}) = -1 \quad \text{for} \quad |\hat{u}| = 1\,, \tag{12}$$
$$\Delta_{\mathrm{adim}}(\hat{u}) = 0 \quad \text{for} \quad |\hat{u}| \geq 2\,. \tag{13}$$

The complete function is plotted in the inset of Fig. 2.

As a self-consistent validation of our procedure, we evaluated numerically the correlator $\Delta_\xi(u)$, and as shown in Fig. 2 we find an excellent agreement with the expression (10).

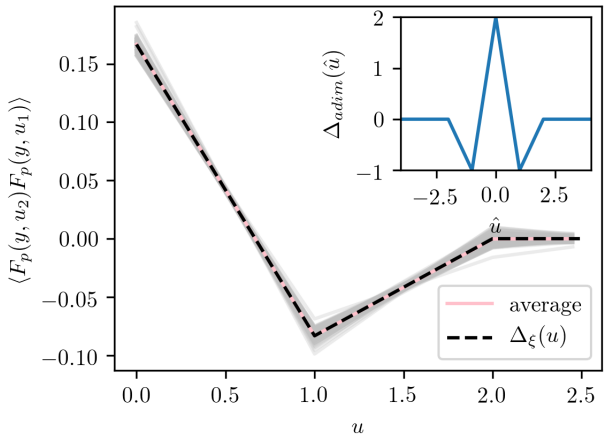

Figure 2. Numerical evaluation of the pinning force correlator for 100 different disorder realizations with $\epsilon = 1$ (gray lines) and its average (pink). In black dashed line we show $\Delta_\xi(u)$, the expected correlator given by Eq. (10) with $D_0 = 1/12$. In the inset, we show the adimensionalized force correlator $\Delta_{\mathrm{adim}}(\hat{u})$ connecting the values of Eqs. (11)-(13).

C. Correlators in Fourier space and disorder strength

One can check that $\int_{\mathbb{R}} \mathrm{d}\hat{u}\, \Delta_{\mathrm{adim}}(\hat{u}) = 0$, as expected for the 'random-bond' disorder we consider. To access the disorder strength D, we switch to Fourier space where we can more easily exploit the relation between the correlators $\Delta_\xi(u) = -DR''_\xi(u)$ from Eq. (1).

We first rewrite, similarly to Eq. (10), the random potential correlator in terms of its adimensionalized version, starting from its very definition

$$\overline{U(u)U(0)} \equiv DR_\xi(u) \equiv \frac{D}{\xi} R_{\mathrm{adim}}(u/\xi)\,. \tag{14}$$

First, by direct comparison with the definition in Eq. (4) we can establish its relation to the variance D_0:

$$D_0 \equiv \overline{U(0)^2} = DR_\xi(u=0) = \frac{D}{\xi} R_{\rm adim}(\hat{u}=0)\,, \quad (15)$$

and secondly the relation between the correlators $\Delta_\xi(u) = -DR''_\xi(u)$ becomes

$$\frac{D_0}{\xi^2}\Delta_{\rm adim}(\hat{u}) = -\frac{D}{\xi^3} R''_{\rm adim}(\hat{u})\,. \quad (16)$$

Defining the Fourier transform along the transverse direction as $\hat{\Delta}_{\rm adim}(\hat{q}) = \int_{\mathbb{R}} {\rm d}\hat{u}\, e^{i\hat{q}\hat{u}} \Delta_{\rm adim}(\hat{u})$, one finds by direct computation that it takes the simple form:

$$\hat{\Delta}_{\rm adim}(\hat{q}) = 16 \frac{\left[\sin\frac{\hat{q}}{2}\right]^4}{\hat{q}^2}\,. \quad (17)$$

Defining similarly the Fourier transform $\hat{R}_{\rm adim}(\hat{q}) = \int_{\mathbb{R}} {\rm d}\hat{u}\, e^{i\hat{q}\hat{u}} R_{\rm adim}(\hat{u})$, Eq. (16) rewrites

$$\hat{\Delta}_{\rm adim}(\hat{q}) = \frac{D}{D_0\xi}\hat{q}^2 \hat{R}_{\rm adim}(\hat{q})\,. \quad (18)$$

At this point, we might think that we have some freedom to define $\hat{R}_{\rm adim}$ up to an arbitrary constant, but we have in fact to enforce the imposed normalization $\int_{\mathbb{R}} {\rm d}u\, R_{\rm adim}(\hat{u}) = 1$ or equivalently $\hat{R}_{\rm adim}(\hat{q}=0) = 1$. This is achieved by imposing $\frac{D}{D_0\xi} = 1$ and thus

$$\hat{R}_{\rm adim}(\hat{q}) = 16\frac{\left[\sin\frac{\hat{q}}{2}\right]^4}{\hat{q}^4} \quad \Rightarrow \quad \lim_{\hat{q}\to 0} \hat{R}_{\rm adim}(\hat{q}) = 1\,. \quad (19)$$

Furthermore, we have by inverse Fourier transform:

$$R_{\rm adim}(\hat{u}=0) = \int_{\mathbb{R}} \frac{{\rm d}\hat{q}}{2\pi}\, \hat{R}_{\rm adim}(\hat{q}) = \frac{2}{3}\,. \quad (20)$$

We have, at last, directly access to the disorder strength:

$$D \overset{(15)}{=} \frac{D_0\xi}{R_{\rm adim}(\hat{u}=0)} \overset{(20)}{=} \frac{3}{2} D_0\xi\,. \quad (21)$$

The last expression is valid for any random potential generated by a linear interpolation between uncorrelated random points, drawn from an arbitrary distribution $\mathcal{P}(U_k)$ with zero mean and variance D_0. For the uniform distribution we consider, Eq. (4) implies

$$D^{\rm uniform} = \frac{3}{2} D_0\xi = \frac{1}{8}\epsilon^2\,. \quad (22)$$

II. PARAMETERS OF NUMERICAL SIMULATIONS

To solve the quenched Edwards-Wilkinson equation (Eq. (1) of the main text) and compute the interface roughness, we take advantage of massively parallel accelerated computing with a CUDA C++ code running in NVIDIA GPUs with a Volta architecture, in double precision. At each simulation step we approximate the second derivative of u along the y-direction by a two-point central finite difference scheme and integrate in time with a first-order Euler step. Pseudo-random numbers are generated with a counter-based RNG (Philox, allowing 2^{64} parallel and distinct streams with a period of 2^{128} [1]). For the thermal noise, we use Gaussian distributed numbers while for the quenched disorder, we use the method described in Sec. I (and in Sec. III in the consistency check described in the same section): the method consists in a linear interpolation of uniformly distributed random numbers with the implementation proposed in [2]. These random numbers, uncorrelated from site to site, are dynamically generated along the evolution of the interface, *i.e.* we build the disorder at larger u only if the interface has locally wandered further away.

Space discretization along the y-direction is set to 1 and time discretization to 10^{-2}. We can simulate 4 realizations of systems of 512 sites for 10^8 steps in approximately 8 hours. These scheme and parameters give roughness functions in the clean case which are in very good agreement with the theoretical prediction (Eq. (4) in the main text). The corresponding roughness of the simulated systems differs from the theoretically predicted values in less than 10^{-4} for $r \leq 50$ and less than 10^{-3} for larger values of r (both, simulated and predicted roughness functions are shown in Fig. 1 in the main text). This excellent agreement is a strong consistency check that provides a good support for the validity of the numerical procedure in the disordered case.

III. DISORDER GENERATED FROM A GAUSSIAN DISTRIBUTION

For the temperature $T = 0.01$, we determined the excess roughness $B^{\rm Gauss}_{\rm dis}(r)$ for a disorder potential where the U_i's are distributed with a Gaussian distribution with the same variance $\overline{(U_i)^2} = 1/12$ as the uniform one, see Eq. (4). On Fig. 3, $B^{\rm Gauss}_{\rm dis}(r)$ is compared to the excess roughness $B_{\rm dis}(r)$ computed –as in the rest of the paper– for a disordered potential with the U_i's drawn from a uniform distribution, as described in section I.

The results show that $B^{\rm Gauss}_{\rm dis}(r)$ is very close to $B_{\rm dis}(r)$. This provides a strong evidence supporting the following points: in the asymptotic regime $r \to 0$, the power-law behaviour $B_{\rm dis}(r) \sim r^{2\zeta_{\rm dis}}$ is universal, *i.e.* presents an exponent $\zeta_{\rm dis}$ which does not depend on the specific random-potential disorder distribution. This is an important aspect, as the asymptotic regime $r \to 0$ where $B_{\rm dis}(r)$ presents the power-law behaviour $\sim r^{2\zeta_{\rm dis}}$ could have been sensitive to the details of the disorder correlator at small scales. Also, the prefactor A in $B_{\rm dis}(r) \sim A\, r^{2\zeta_{\rm dis}}$ is mainly governed by the variance D_0 of the disorder distribution (which is the same in the uniform and in the Gaussian distribution we have used

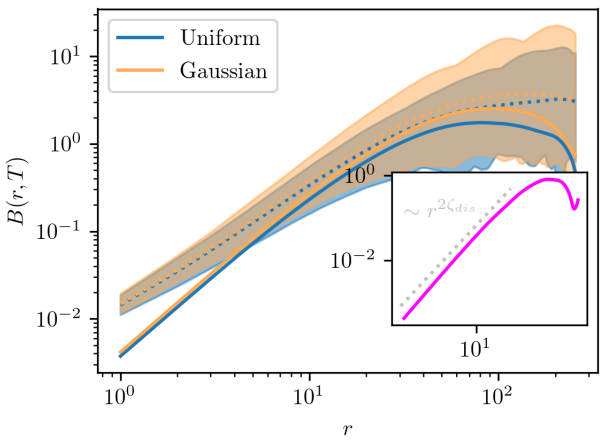

Figure 3. Roughness (dotted lines) and excess roughness (continuous lines) at $T = 0.01$ averaged over 50 realizations with increased statistics, obtained for disorders generated from a uniform and a Gaussian distribution. In the inset we show the difference between both excess roughness.

for $\mathcal{P}(u)$). Last, we expect also that this prefactor A depends, through a numerical constant, on the rescaled shape $\Delta_{\rm adim}(\hat{u})$ of the disorder correlator. This is seen in the small difference $|B_{\rm dis}^{\rm Gauss}(r) - B_{\rm dis}(r)| \ll B_{\rm dis}(r)$ shown in the inset of Fig. 3. Such difference also scales as $r^{2\zeta_{\rm dis}}$ in the asymptotic regime $r \to 0$, indicating that indeed only the prefactor A is affected by the adimensionalized shape of the disorder correlator.

IV. SCALING OF THE CROSSOVER SCALE $r_1(T)$

The crossover scale r_1 is determined numerically by the intersection between the two power-law scalings $B_{\rm dis}(r) \sim r^{2\zeta_{\rm dis}}$ and the thermal regime Tr/c. The scaling arguments presented in the main text indicate that r_1 scales with temperature as

$$r_1(T) \sim \begin{cases} T^{1/[1-2(1-\zeta_{\rm dis})]} & \text{for } T \ll T_c\,, \\ T^5 & \text{for } T \gg T_c\,. \end{cases} \qquad (23)$$

To determine how our numerical results are compatible with such predictions, we have used a fitting function

$$r_1^{\rm fit}(T) = C\,T^{\alpha_-}\left[1 + (T/T^\star)^{\alpha_+ - \alpha_-}\right] \qquad (24)$$

(where C and $T^\star$ are constants and $\alpha_- < \alpha_+$) that interpolates between the regimes $r_1^{\rm fit}(T) \sim T^{\alpha_-}$ for $T \ll T^\star$ and $r_1^{\rm fit}(T) \sim T^{\alpha_+}$ for $T \gg T^\star$. The prediction of Eq. (23) corresponds to

$$\alpha_+ = 5\,, \quad \alpha_- = 1/[1 - 2(1 - \zeta_{\rm dis})]\,. \qquad (25)$$

A first scenario where $\zeta_{\rm dis} = \zeta_{\rm dis}^{\rm th} = 1$ (according to the perturbative analysis of [3], for instance) corresponds to $\alpha_- = 1$. A second scenario where $\zeta_{\rm dis} \approx 0.9 < 1$ corresponds to $\alpha_- \approx 1.25 > 1$. To distinguish between these two possibilities, we have fitted the values of $r_1(T)$ obtained numerically with the function (24), where we fixed the exponent $\alpha_\pm$ and we left the constants C and $T^\star$ as free parameters. As shown on Fig. 4, the data provide a strong evidence supporting the second scenario $\zeta_{\rm dis} \approx 0.9 < 1$. Also, leaving α_- as a free parameter for the fit, one finds $\alpha_- \approx 1.33$ which corresponds to the value $\zeta_{\rm dis} \approx 0.88$: it is compatible with the value $\zeta_{\rm dis} \approx 0.91$ obtained in the main text with a completely different method.

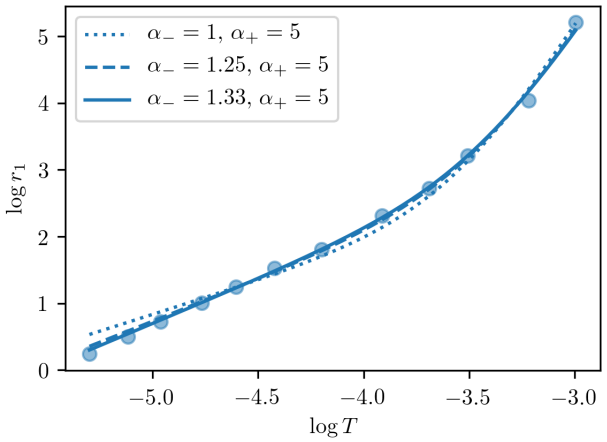

Figure 4. Behaviour of the crossover scale $r_1(T)$. The points are the result of numerical simulations, while the dashed and full line curves correspond to the two scenarios discussed in the text. The exponent $\alpha_- \approx 1.25 > 1$ is more compatible with the numerical data, and corresponds to $\zeta_{\rm dis} \approx 0.9 < 1$.

V. DETERMINATION OF THE BEST VALUE OF $\zeta_{\rm dis}$

To obtain $\zeta_{\rm dis}$ from the numerical data presented in the main text, we fit $B_{\rm dis}(r,T)$ independently for each value of T in the range $r = [1, r_f]$. For the nine lowest temperatures we have studied, we find values of $\zeta_{\rm dis}$ between 0.9 and 0.92. To determine the best value of this exponent that is compatible with every temperature we considered, we rely on the following scaling argument. We predict that $B_{\rm dis}(r_0,T)/r_0^{2\zeta_{\rm dis}}$ should be independent of r_0 for all temperatures T. In Fig. 5, we illustrate that the best choice of $\zeta_{\rm dis}$ that ensures this collapse is $\zeta_{\rm dis} = 0.91 \pm 0.01$. We quantify the spread of the functions $B_{\rm dis}(r,T)/r^{2\zeta_{\rm test}}$ around their mean value for different values of $\zeta_{\rm test}$ by computing the function $F_{T,r}(\zeta) = \Sigma_{T,r}\left(\frac{B_{\rm dis}(r,T)/r^{2\zeta} - \Sigma_{r_i} B_{\rm dis}(r_i,T)/r_i^{2\zeta}}{\Sigma_{r_i} B_{\rm dis}(r_i,T)/r_i^{2\zeta}}\right)^2$ with $r_i = 1, \ldots, 5$, for the 5 lowest studied temperatures. The resulting function has a minimum in $\zeta = 0.91$, as shown in the inset of Fig. 5.

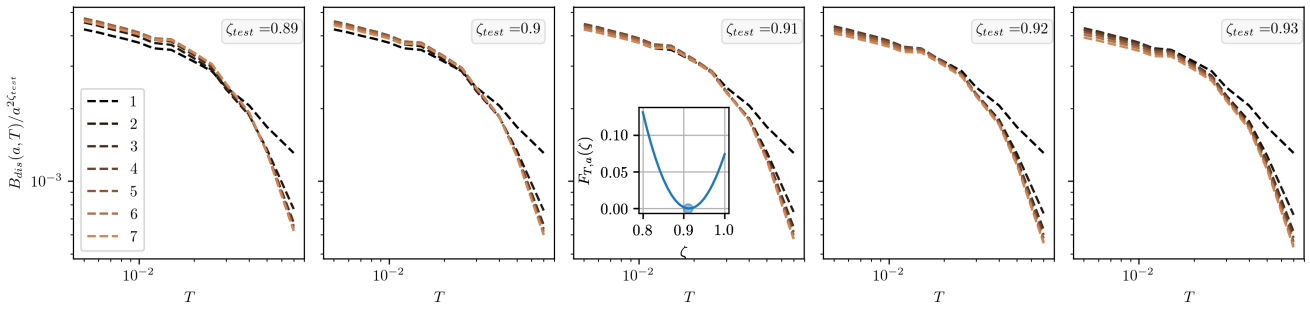

Figure 5. Numerical collapse of the excess roughness, described in the text, for values ζ_{test} of ζ_{dis} ranging from 0.89 to 0.93. The value achieving the best collapse is $\zeta_{\text{dis}} = 0.91$. At 0.91 the function $F_{T,a}(\zeta)$ (see text) has a minimum, as shown in the inset. The different dashed lines correspond to the value of a indicated in the caption.

[1] J. K. Salmon, M. A. Moraes, R. O. Dror, and D. E. Shaw, Parallel random numbers: as easy as 1, 2, 3, in *Proceedings of 2011 International Conference for High Performance Computing, Networking, Storage and Analysis* (2011) pp. 1–12.

[2] E. E. Ferrero, S. Bustingorry, and A. B. Kolton, Non-steady relaxation and critical exponents at the depinning transition, Phys. Rev. E **87**, 032122 (2013).

[3] S. E. Korshunov, V. B. Geshkenbein, and G. Blatter, Finite-temperature perturbation theory for the random directed polymer problem, Journal of Experimental and Theoretical Physics **117**, 570 (2013).